Ceramics International 42 (2016) 12630–12638

Contents lists available at ScienceDirect

Ceramics International

journal homepage: www.elsevier.com/locate/ceramint

Role of spin-glass phase for magnetoresistance enhancement in nickel substituted lanthanum calcium manganite

Akash Yadav [a], Jyoti Shah [b], Rekha Gupta [a], Ajay Shukla [a], Sukhvir Singh [a], R.K. Kotnala [a,*]

[a] CSIR-National Physical Laboratory, New Delhi 110012, India
[b] CSIR-NPL, India

ARTICLE INFO

Article history:
Received 3 March 2016
Received in revised form
21 April 2016
Accepted 27 April 2016
Available online 3 May 2016

Keywords:
Ni substituted LCMO
Spin-glass phase
Low temperature magnetoresistance
Double exchange interaction
Spin tunneling

ABSTRACT

Effect of Ni substitution in lanthanum calcium manganite (LCMO) has been investigated for change in magnetoresistance (MR). Scanning electron microscopy images revealed decrease in grain size from 3.72 μm to 0.55 μm by Ni substitution. Maximum increase in MR has been found 28% at low temperature (100 K) for $x=0.10$, Ni substitution at Mn site. Metal insulator transition temperature has been decreased from 253.2 K for $x=0.0$–90 K for $x=0.10$. Above $x=0.10$, Ni substitution no metal-insulator transition temperature appeared due to the presence of porosity in the samples. Ni substitution lowered the magnetic transition temperature from 255 K for $x=0.0$–125 K for $x=0.25$. Lowering of irreversible temperature (T_{irr}) from 250 K for $x=0.0$–135.4 K for $x=0.20$ has been obtained by zero field cooled (ZFC) and field cooled (FC) measurements confirm reduction of ferromagnetic clusters and spin-glass phase like behavior due to Ni presence. The spin-glass phase presence allows spin-polarized tunneling even at low magnetic field, which ultimately results in enhancement of MR at low temperature. Core level X-ray photoelectron spectroscopy measurements confirm Ni^{2+} charge state of Ni ions and increase in Mn^{4+}/Mn^{3+} ratio with increasing Ni content. Increase in resistivity and weakening of ferromagnetism with Ni substitution at Mn site has been observed due to the reduction in grain size and dilution of double exchange interaction.

1. Introduction

Rare earth manganites of general formula $R_{1-x}A_xMnO_3$ (R = rare earth element, A = Sr, Ba, Ca) have attracted scientific interest for many decades[1,2]. The structural, magnetic and transport properties of $R_{1-x}A_xMnO_3$ have been widely explored in past [3–6]. These materials have novel physical properties and potential applications in magnetic-field sensor, read head, spintronics, microwave, magneto caloric devices, solid oxide fuel cells and biomedical application in treating cancer tumors [7–10]. Doping effect of transition metal ions (viz. Fe, Cr, Ni, Cu, Co, Zn, Al etc.) in $R_{1-x}A_xMnO_3$ system at the Mn site has been studied extensively [10–21]. Small change in double exchange interaction (Mn^{3+}–O–Mn^{4+}) due to the Ni^{2+} ion substitution resulted into large change in magnetic and transport properties of such systems [17]. Increase in MR has been reported in Ni doped $La_{0.67}Sr_{0.33}MnO_3$ system at low temperature [10,21]. Nickel substitution at Mn site weakens ferromagnetism and increases the resistivity in manganite system [22,23]. Ni doping at Mn site suppresses both Curie and metal-insulator transition temperatures. It also weakens the long range ferromagnetic ordering and induces smaller spin-glass system which influences the low temperature MR in the $La_{0.7}Sr_{0.3}MnO_3$ system [24]. There are very few reports on magnetoresistance enhancement in Ni substituted LCMO [20,25]. In the present work, Ni substituted $La_{0.7}Ca_{0.3}Mn_{1-x}Ni_xO_3$ ($x=0.0$, 0.02, 0.05, 0.10, 0.15, 0.20, and 0.25) samples have been prepared by solid state reaction method, and their magnetic and magneto transport properties have been investigated systematically. It has been observed that Ni substitution at Mn site weakens the long-range ferromagnetic ordering and spin-glass phase increased that influences the low field and low-temperature MR%. The system has been mainly explored for spin-dependent tunneling among the randomly oriented spin-glass groups, scattering at grain boundaries and double exchange interaction.

2. Experimental

Nickel substituted $La_{0.7}Ca_{0.3}Mn_{1-x}Ni_xO_3$ ($x=0.0$, 0.02, 0.05, 0.10, 0.15, 0.20, and 0.25) sample series has been prepared by solid-state reaction method. Solid-state reaction method has been used to obtain good quality polycrystalline dense samples [10].

* Correspondence to: Multiferroic & Magnetics, CSIR-NPL, India.
E-mail addresses: rkkotnala@nplindia.org, rkkotnala@gmail.com (R.K. Kotnala).

http://dx.doi.org/10.1016/j.ceramint.2016.04.162
0272-8842/

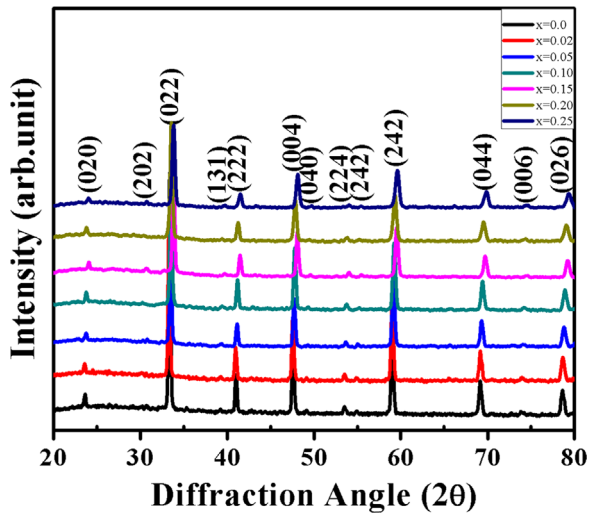

Fig. 1. XRD patterns for $La_{0.7}Ca_{0.3}Mn_{1-x}Ni_xO_3$ ($0 \le x \le 0.25$) series.

Precursors La_2O_3, MnO_2 (Alfa Aesar 99.9% purity), NiO (Alfa Aesar purity 99%), and $CaCO_3$ (John Baker 99.5% purity) were taken in stoichiometric ratio and grinded with agate pastel mortar for 1 h. Homogenized powder was calcined at 900 °C for 18 h in air. Calcined powder was pelletized using polyvinyl acetate (PVA) as a binder. Pellets were sintered at 1300 °C for 24 h followed by slow cooling in air. The crystalline structure of the samples was evaluated by X-ray diffractometer (Brukar D-8 Advanced Diffractometer) with CuK_α ($\lambda = 0.154$ nm) radiation. X-ray photoelectron spectroscopy (XPS) measurements were performed using an ultra high vacuum (UHV) multi-probe surface analysis system from Omicron nanotechnology GmbH, Germany equipped with EA 125 electron analyzer and monochromatic Al Kα and non-monochromatic dual anode (Mg Kα, Al Kα) X-ray source. Base pressure of the experimental chamber was 3×10^{-11} Torr. All binding energies have been referenced to the Fermi edge of an Ar^+ sputtered clean polycrystalline Ag sample. C 1s core level binding energy (BE) (284.8 eV) was used to correct any small shift due to charging. The resistivity of the sample series was measured by four-probe method. Curie temperature and magnetization measurements of samples were performed on vibrating sample magnetometer (VSM, Lakeshore 7304). Temperature dependent resistivity (ρ) measurements have been carried out in closed cycle refrigerator equipment in absence of magnetic field. Surface morphology and grain size distribution of the sample series was analyzed by scanning electron microscopy (EVO MA10 VPSEM) and transmission electron microscope (FEI model TF30). The MR% of the sample series at 100 K was observed with magnetic field upto 8800 Oe (Bruker electromagnet), by applying a constant current of 1 mA (dc current source, Keithley 6221) and corresponding voltage obtained by nanovoltmeter (Keithley 2182A).

3. Results and discussion

3.1. X-ray diffraction (XRD)

Crystal structure of pure and Ni incorporated LCMO has been analyzed from X-ray diffraction (XRD) patterns taken for 2θ range from 20° to 80° as shown in Fig. 1. XRD patterns confirm single phase formation of perovskite structure with Ni content in LCMO. Lattice parameter and volume of perovskite unit cell has been obtained by fitting Rietveld refinement with goodness of fit, χ^2 value below 5 for $x = 0.0$ and 0.15 samples are shown in Fig. 2. Ni substituted LCMO shows orthorhombic distorted ABO_3 type perovskite structure with space group P_{bnm} without any secondary or impurity phase formation. The lattice constants and unit cell volume of pure LCMO have been found to decrease with increasing Ni concentration as shown in Fig. 3. The decrease in unit cell volume with Ni doping can be attributed to smaller ionic radii of Ni^{2+} ion (0.56 Å) replacing Mn^{3+} ion (0.64 Å) site. The unit cell volume of sample series has been given in Table1.

3.2. X-ray photoelectron spectroscopy (XPS)

XPS core level measurements have been utilized to identify valance state of Ni ion and Mn^{4+}/Mn^{3+} ionic ratio present in $La_{0.7}Ca_{0.3}Mn_{1-x}Ni_xO_3$ ($x = 0.0$, 0.1, and 0.25) samples. Mixture of Gaussian and Lorentzian (mostly Gaussian) peaks has been used to fit the core level spectra. Shirley method has been used to remove secondary electron background [26]. The Mn 2p and 3p XPS core level spectra of pristine and Ni substituted LCMO samples are shown in Fig. 4. Analysis of Mn 2p and 3p core level spectra revealed mixed valence state of Mn ions in pristine and Ni incorporated samples. It has been found that contribution of Mn^{4+} ions increased compared to Mn^{3+} ions with Ni incorporation [27–29]. This was further confirmed by calculated ratio of Mn^{4+}/Mn^{3+}

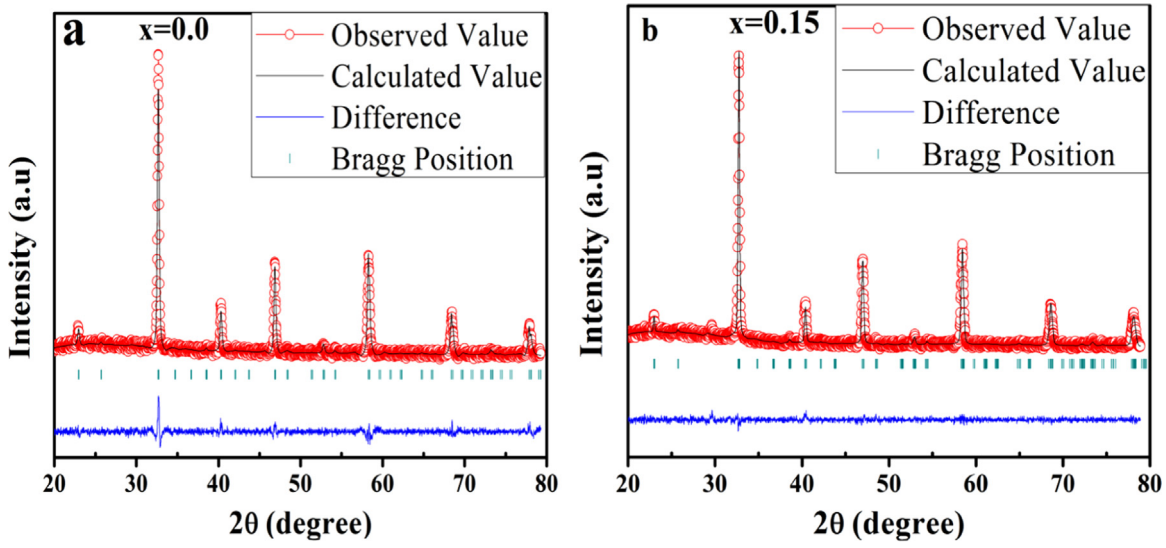

Fig. 2. Rietveld fitted XRD patterns of $La_{0.7}Ca_{0.3}Mn_{1-x}Ni_xO_3$: (a) $x = 0.0$ and (b) $x = 0.15$ samples.